

E. J. Stamhuis · B. Dauwe · J. J. Videler

How to bite the dust: morphology, motion pattern and function of the feeding appendages of the deposit-feeding thalassinid shrimp *Callinassa subterranea*

Received: 26 September 1997 / Accepted: 27 March 1998

Abstract The morphology of the mouthparts of *Callinassa subterranea* (Montagu, 1808) was studied using light microscopy and scanning electron microscopy. All the mouthparts except the mandible, but including the mandibular palp, appeared to be supplied with a wide variety of setae. The setae of the medial rims of these appendages (the “ventral screens”) show a trend of decreasing passive motility towards the oral side; this applies to the setae themselves as well as the microstructures on the setae. The motion of the mouthparts was filmed from aboral and rostral views with macro-video and endoscopy equipment, after marking the joints and tips of maxillipeds and the mandibles. Motion analysis showed that all mouthparts except the first maxilla (Mx1) actively moved during deposit feeding. The first and second maxillipeds (MP1, MP2), Mx2 and the mandibles moved at the same frequency, contralateral in phase, but with a 50% phase shift between ipsilateral mouthparts. The MP3 moved at a lower frequency with a contra-lateral phase shift of about 50% without an obvious phase relation with the other mouthparts. According to the following scenario, the feeding mechanism of *C. subterranea* seems to be based on the morphology and motion of the appendages in combination with specific setal functions. The MP3 make large excursions over the substrate, suspending the sediment in front of the MP2. The MP2 move through the upper layer of the suspension, trapping particles of 30 µm and smaller. These particles are combed out by the MP1 and transferred to the mouth opening by the cascade of finely structured setae of the inner mouthparts, and finally ingested.

Introduction

Deposit-feeding benthic decapods generally ingest sediment particles and digest the organic coating of these particles (Fenchel 1972; Dale 1974). Deposit or sediment is commonly processed and sorted during foraging, and only a fraction is ingested (Lopez and Levington 1987). The organic content of sediment and detrital particles depends on grain size, surface structure and density (Weise and Rheinheimer 1978; Robertson and Newell 1982a,b; Taghon 1982). Small particles contain relatively more organic coating due to a higher surface-to-volume ratio compared to larger particles. Optimal foraging, yielding the highest energy input per unit of time, requires a deposit feeder to mainly select the smallest particles (Taghon et al. 1978). Studies on deposit feeding in semaphore crabs (*Uca* sp.) ghost shrimps (*Ocyropsis* sp.) and hermit crabs (*Pagurus* sp.) showed that they indeed select and ingest the small-grain fraction (Altevogt 1957; Miller 1961; Roberts 1968; Fenchel 1972; Greenwood 1972; Fielder and Jones 1978; Khan and Natarajan 1981; Robertson and Newell 1982a, b; Schembri 1982a, b; Alexander and Hindley 1985). Details of the selection mechanisms usually remain unclear, due to the high motion frequencies of the mouthparts during feeding and the lack of appropriate recording methods. In several studies on decapod deposit feeding, some mouthparts were amputated to get a clearer view of others during feeding (Miller 1961; Robert 1968; Schembri 1982a; Skilleter and Anderson 1986). The conclusions regarding natural feeding behaviour and feeding mechanisms based on this type of study can be questioned (Altevogt 1976).

The morphology of the mouthparts of decapods commonly deviates strongly from the standard crustacean biramous configuration. The maxillae (Mx), essentially being modified protopods, are usually dorso-ventrally flattened with pronounced endites. Of the larger maxillipeds (MP), only the endopodites show a pediform appearance (Manton 1964, 1977). Not only the

Communicated by O. Kinne, Oldendorf/Luhe

E.J. Stamhuis (✉) · B. Dauwe · J.J. Videler
Department of Marine Biology,
University of Groningen, P.O. Box 14,
9750 AA Haren, The Netherlands

macro-morphology but also the micro-morphology of the mouthparts, mainly determined by the setal structures, is related to the feeding mechanism in decapods (Wagner and Blinn 1987; Jacques 1989). The structure of the setae is probably as diverse as their proposed functions (Thomas 1970, 1973; Factor 1978; Gemmell 1979; Pohle and Telford 1981). Besides functioning as mechanical effectuators during foraging (Gemmell 1979; Jacques 1989; Watling 1989), setae may also function as receptors of chemical, mechanical, thermal or light stimuli (Shelton and Laverack 1970; Wiese 1976; Derby 1982, 1989; Gleeson 1982). Classification systems have been developed for setae, based on morphological characteristics (Jacques 1989) as well as on homology (Watling 1989). The assumed functions of most seta types are still ambiguous, possibly because setae can sometimes serve more than one purpose (Pohle and Telford 1981). Setae presumably functioning as effectuators during deposit feeding have been studied in littoral crabs (Altevogt 1976; Pohle and Telford 1981; Schembri 1982a,b; Maitland 1990) and in lobsters (Farmer 1974; Factor 1978). The mouthpart morphology in relation to the feeding mechanism of the endobenthic thalassinids, including deposit-feeding callianassids (Griffis and Suchanek 1991; Nickell and Atkinson 1995), has received little attention so far.

Callianassa subterranea, a benthic endofaunal thalassinid which is highly abundant in the central North Sea (de Wilde et al. 1984), is a deposit feeder spending almost 40% of its active time burrowing, and processing sediment (Stamhuis et al. 1996). This species ingests only a certain fraction of the excavated sediment. The organic content of this fraction is up to ten times as high as that of a random sediment sample, indicating a selection mechanism (Stamhuis et al. 1998). However, the morphology and function of the feeding apparatus are still unclear. The present study therefore concentrates on the macro- and micro-morphology of the mouthparts, their motion patterns and their function during feeding, to obtain insight into the mechanism of deposit feeding and sediment sorting in *C. subterranea*, as well as in other deposit-feeding decapods.

Materials and methods

Collection and preparation

Callianassa subterranea (Montagu, 1808) were collected at the southern border of the Oyster Grounds and at the Frisian Front, central North Sea, around 53°45'N; 4°30'E. Sampling trips were made in June 1990 and October 1991 with the Dutch research vessel "Aurelia" (Stamhuis et al. 1996). Undamaged shrimp were stored in artificial seawater aquarium systems in the laboratory, in 5- or 10-litre containers nearly filled with sediment from the sampling area. Slightly damaged individuals (e.g. missing the large cheliped or a pereopod) were kept for morphological studies; these shrimps were immediately sacrificed on board using a 12% formaldehyde solution, and stored in seawater with 4% formaldehyde.

The morphology of the mouthparts was studied under a dissection microscope. Detailed pictures were obtained by scanning electron microscopy (SEM), after applying critical point drying and

sputter coating. Primary emphasis was put on details of the appendages situated aborally of the mouth opening, mainly involved in food processing. The terminology used for the appendages, their segments and their outgrowths is derived from Manton (1964, 1977). Setae were classified according to the nomenclature used by Jacques (1989) and Watling (1989), based on Thomas (1970, 1973).

Motion analysis

To observe and film the motions of the feeding appendages, an experimental animal was kept in a Perspex burrow inside a temperature-controlled (12 °C) aquarium. The burrow was designed as a U-shaped tube with two turning chambers (Stamhuis et al. 1997). Video pictures of the moving appendages were taken from a ventral perspective using a high resolution camera with a macro lense. A rostral view was obtained by attaching a video camera to a rigid endoscope. The endoscope entered the horizontal tube of the Perspex burrow through a hole in the tube wall. Filming and observations were carried out under red light conditions ($\lambda > 600$ nm), to which the shrimp showed no visible reaction.

To be able to follow the movements of single appendages, the maxillipeds were marked after anaesthetizing the animals by cooling them down to 1 °C. The mouthparts were dried with a tissue and the tips and joints of MP2 and MP1 were marked with permanent ink using a blue felt pen with a sharpened tip. Video recordings from the ventral side were taken of eight individuals.

In the rostral view, the large cheliped often hampered observation and filming of the feeding appendages. Video frames of three individuals were taken from this side. A clear view of the mouthparts was obtained for an animal which accidentally lost its large cheliped during handling. This cheliped is not involved in food processing. Comparison with the motion patterns of intact shrimp showed that the missing cheliped did not affect the movements of the mouthparts.

To induce foraging behaviour and food processing, experimental animals were starved for at least 48 h before being introduced into the artificial burrow. After a short acclimatization period, provision of a thin layer of sediment in the horizontal tube induced immediate foraging behaviour. Only motion patterns including motion of the mandibles were characterized as feeding.

The marked points and the medial rims of the mandibles were located on each of the digitized video images. By accessing each of the two separate fields per video image, the temporal resolution of the motion analysis was 0.02 s, corresponding with 50 images per second. The stored coordinates were later used to follow single points in time to study interactions between the separate mouthparts. The coordinates were also used to visualize the appendages as wire frames (Fig. 1) on a computer screen. Successive wire frames were used to play back any part of the motion sequence of one appendage or combinations of appendages, at any speed. This provided insight into the paths followed by individual appendages in time.

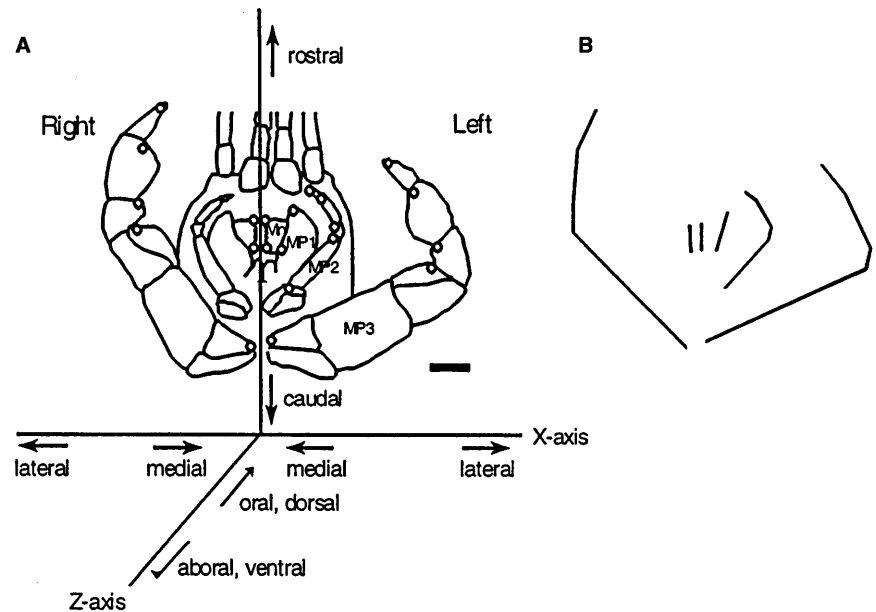
Results

In this section the morphology of all mouthparts is described first, followed by descriptions of the motion patterns during feeding. These descriptions are used to model *Callianassa subterranea*'s feeding mechanism.

Morphology

The mouthparts of *Callianassa subterranea* consist of six paired appendages. From oral to aboral these are: the mandibles, the first and second maxillae, and the first,

Fig. 1 *Callianassa subterranea*. **A** Ventral view of the mouthparts (setae not shown) showing the digitized (marked) points as open circles. The first and second maxillae are masked by the first maxillipeds (MP1). An orthogonal system of reference is added to define orientations and directions of movement of the mouthparts. Scale bar = 1 mm. **B** Wire frame diagram derived from marked points



second and third maxillipeds. These structures are characterized by their position, shape, rami, number of segments, processes, and the presence and morphology of setae, teeth and denticles. The setae are often arranged in parallel rows, usually called “setal screens”. The setal screens ventral from the mouth opening are referred to as the “ventral screens”.

Mandible (Fig. 2)

Each mandible consists of a base carrying two processes and a palp. There is a small molar process orally, and a large incisor process aborally (Fig. 2A,B). The medial rim of the spade-shaped incisor process has 11 or 12 tooth-shaped projections. The palp consists of three segments, and originates anteriorly of the incisor process. It curves to median, the terminal segment ending orally of the incisor process. The aboral side of the terminal segment has no setal coverage, the other sides bear five types of setae. Proximally, the anterior side bears four to six rows of plumo-denticulate setae. These are 200 μm long and 5 μm thick (Type 1) (Fig. 2A,B). Distally, there are four additional types of setae. A few rows of moderately serrulated setae, 70 μm long and 5 μm thick, are situated on the medio-anterior rim of the segment (Type 2). These setae have smooth shafts and a distal serrulation on the aboral side consisting of two rows of denticles (Fig. 2C). On the oral side of the terminal segment of the palp, a few rows of finely serrulated setae are found (Type 3), which are only marginally different from the Type 2 setae. The Type 3 setae have the same diameter as the Type 2 setae (5 μm), but they are longer (100 μm) and the denticles of the serrulation are smaller (Fig. 2D).

Between the Type 2 and the Type 3 setae, the median side of the third segment is covered with strongly ser-

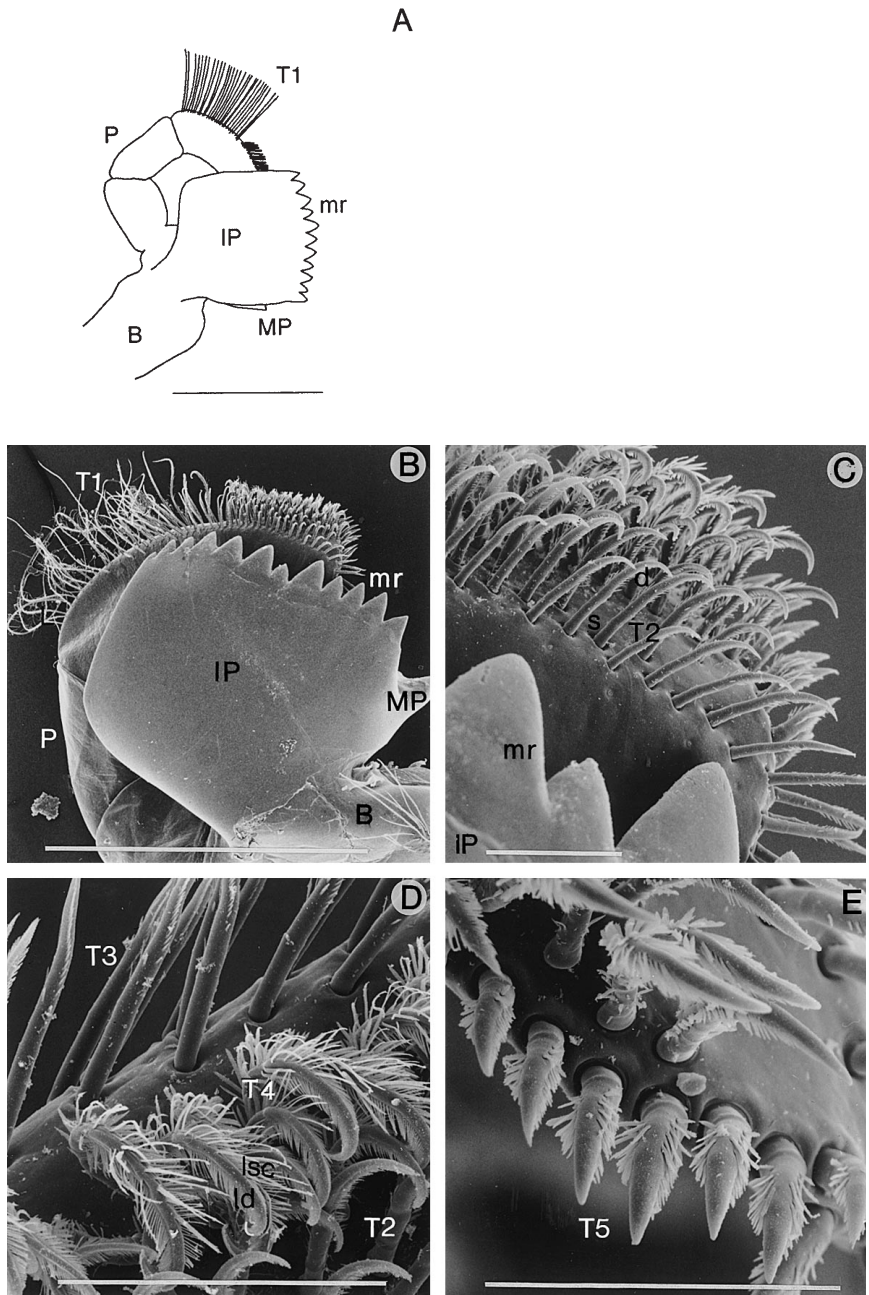
rated setae, approximately 100 μm long and 7 μm thick (Type 4). The serration on the aboral side consists of very long denticles, and the other sides of the setae are covered with long, fingered scales (Fig. 2D). On the distalmost part of the palp, a row of short serrated setae is situated (Type 5). These setae show some similarity with the Type 4 setae but are shorter (30 to 50 μm) and thicker (approximately 10 μm). The serration and the scales are less pronounced (Fig. 2E).

First maxilla (Mx1) (Fig. 3)

The first maxilla consists of a basipodite, a coxopodite and a palp-like endopodite (Fig. 3A,B). The flat spade-shaped basipodite is positioned ventral of the mouth opening. The spoon-shaped coxopodite is attached posterior of the basipodite, on the ventro-caudal side of the mouth opening. The medial ridge of the basipodite bears two rows of blunt, cuspidate, 85 μm long setae with supra-cuticular joints. The diameter at the base is 25 μm . These setae alternate with more slender serrated setae, 100 μm long and 10 μm thick, with infra-cuticular joints. The distances between the setae vary from 30 to 50 μm (Fig. 3C,D). Aborally from the medial ridge, three rows of smaller, 60 to 100 μm long and 8 μm thick, serrated setae with infra-cuticular joints are found (Fig. 3B, E). The anterior and posterior rims of the basipodite have long serrated setae, pointing in medial direction (Fig. 3A,B,C).

The medial rim of the coxopodite bears a few parallel rows of straight setae, 250 μm long and 15 μm in diameter (Fig. 3F). The setae of the aboral rows are toothed with cup-shaped tips and small denticles on the cup-rim (Fig. 3G). The oralmost row exists of serrulate setae covered with rows of scales.

Fig. 2 *Callianassa subterranea*. Morphology of the mandible. **A** Line drawing and **B** SEM picture from the ventral side. **C, D, E** Detailed SEM pictures of the setae. Scale bars = 1 mm (A, B); 100 μ m (C, D, E) (*B* base; *MP* molar process; *IP* incisor process; *mr* toothed medial rim; *P* mandibular palp; *T1–T5* five types of setae; *s* smooth shaft; *d* denticles; *ld* long denticles; *lsc* long scales)



The distal part of the endite is sparsely covered with single long setae, 8 μ m thick and up to 1000 μ m long, on the medial rim only.

Second maxilla (Mx2) (Fig. 4)

The second maxilla is composed of basipodite and a coxopodite with two lobes each, an endopodite originating proximal from the basipodite and a large membranous scaphognatite (Fig. 4A).

The medial rims of all four lobes of the basipodite and the coxopodite are covered with rows of closely

packed, long and stiff setae. These setae have supra-articular joints, and curve in an oral direction (Fig. 4B). The setae on the medial rim of the basipodite are 300 to 400 μ m long. They are about 7 μ m thick and stand about 30 μ m apart. The proximal part of the setal shafts is smooth with a few setules, gradually becoming serrated distally (Fig. 4C). The tips of these setae are somewhat blunt and curved, the denticles of the serrations are oriented in postero-oral direction.

The setae on the medial rim of the coxopodite are of the same size and ordering as those on the basipodite, but their morphology is different. The proximal part of the shaft of these plumo-denticulate setae bears fingered

Fig. 3 *Callianassa subterranea*. Morphology of the first maxilla. **A** Line drawing of an aboral view. **B** SEM picture of the rostro-ventral side. **C** SEM picture of the oral side of the basipodite. **D, E, F, G** Details of the setae. **Scale bars** = 1 mm (A, B, C); 100 μ m (D, E, F); 10 μ m (G) (*Co* coxopodite; *Ba* basipodite; *En* endite; *mr* medial rim; *cu* cuspidate setae; *sr* serrate setae; *ssr* slender serrate setae; *srs* serrulate setae with small scales; *tsc* toothed setae with cup-shaped tips; *d* denticles)

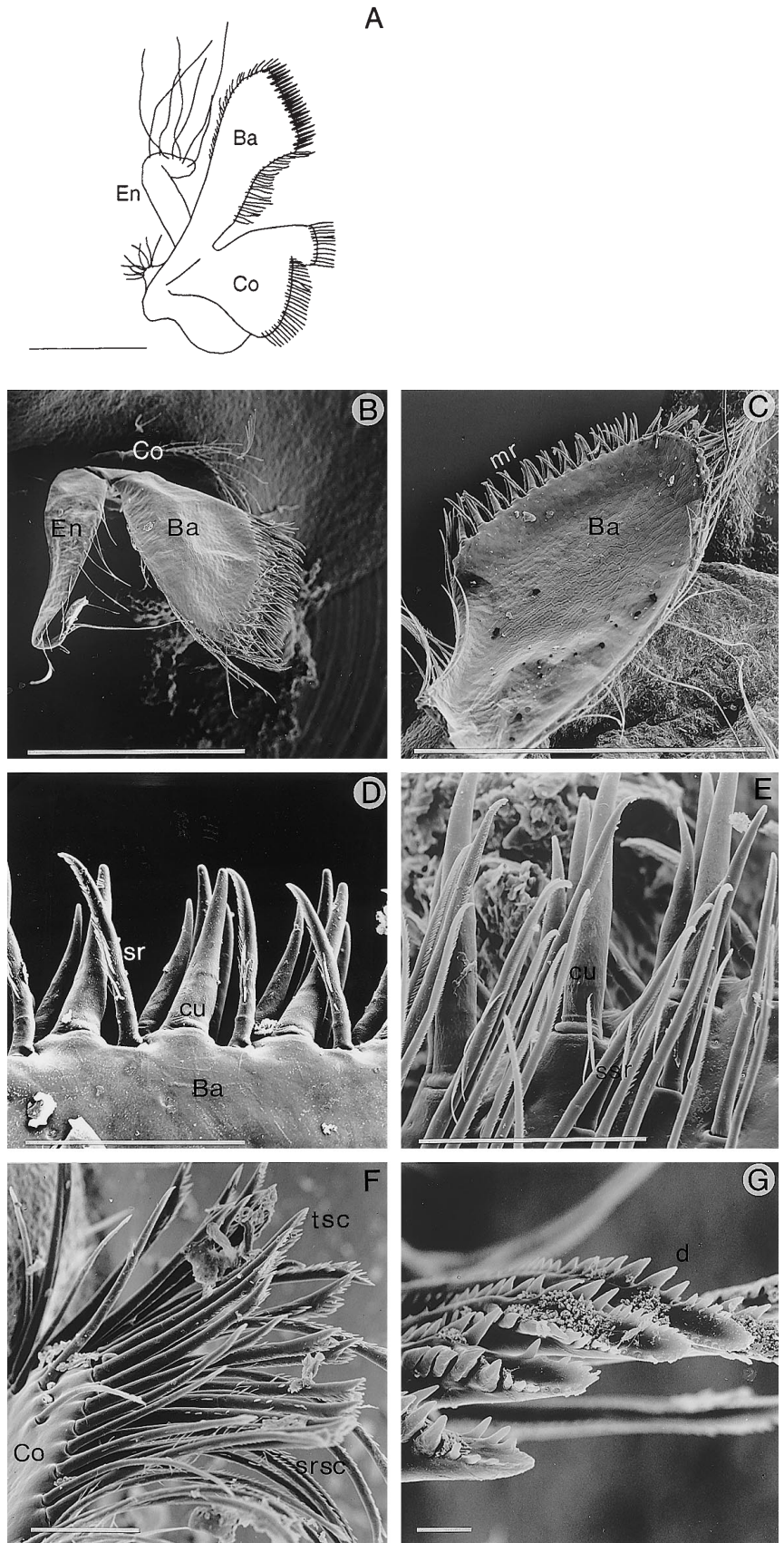
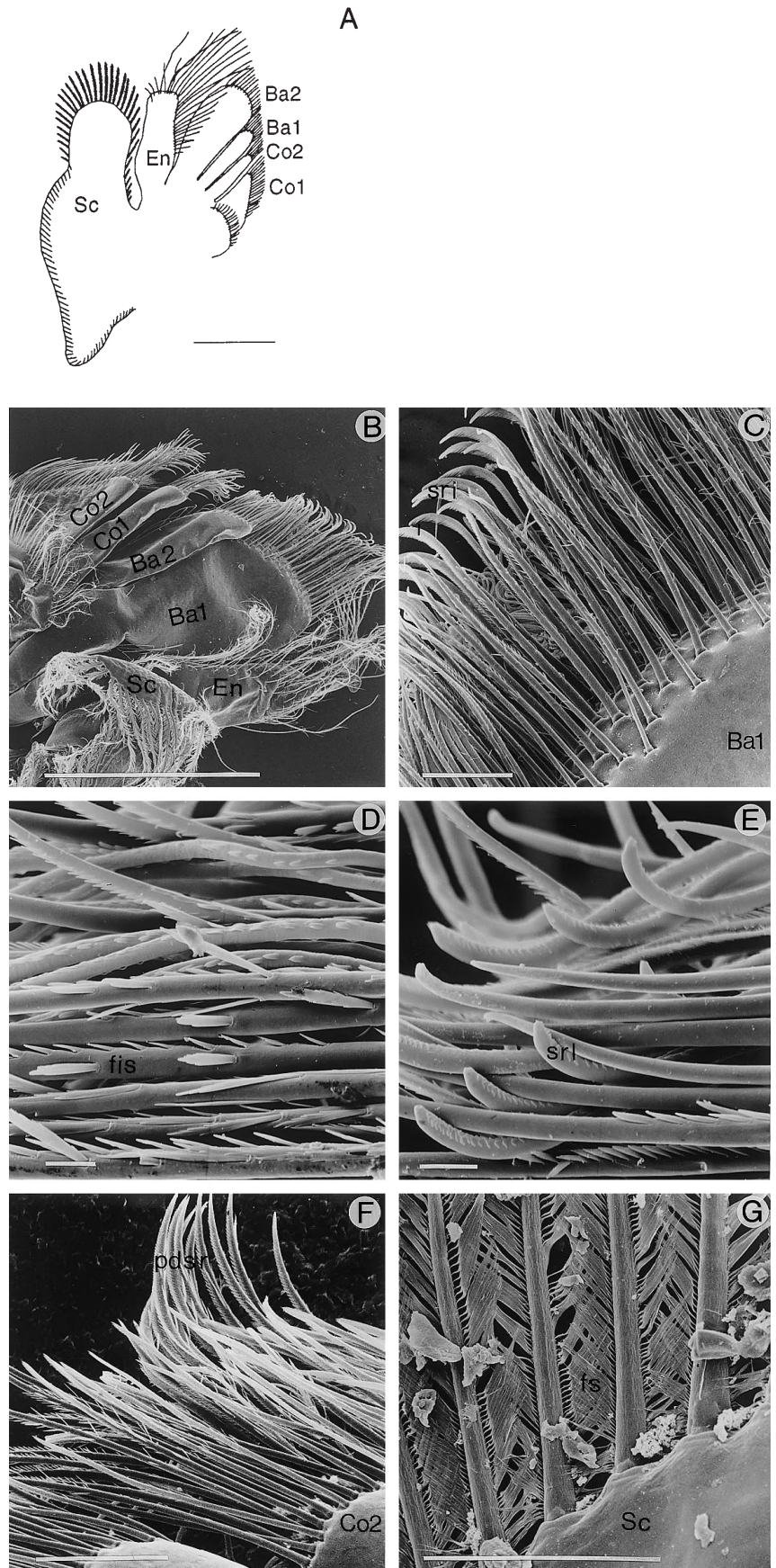


Fig. 4 *Callianassa subterranea*. Morphology of the second maxilla. **A** Line drawing of an aboral view. **B** SEM picture of the rostro-ventral side. **C** View from aboral on basipodital setae. **D** Detail of proximal parts of the coxopodital plumo-denticulate setae. **E** Detail of distal parts of the coxopodital plumo-denticulate setae. **F** Plumo-denticulate setae of the coxal endite (Co2). **G** "Leaf-setae" on the rim of the scaphognatite. *Scale bars* = 1 mm (A, B); 100 μ m (C, F, G); 10 μ m (D, E) (*Co* coxopodite; *Co1*, *Co2* 1st, 2nd lobe of coxopodite; *Ba* basipodite; *Ba1*, *Ba2* 1st, 2nd lobe of basipodite; *En* endite; *Sc* scaphognatite; *sri* setae with increasing serration towards distal; *fis* fingered setules and scales; *srl* serrulated tips; *pdsr* strongly serrated plumo-denticulate setae; *fs* flat setules)



setules of varying size (Fig. 4D), and the distal part is serrulated, although sometimes not very pronounced (Fig. 4E).

The anterior setae of the coxal endite (Co2) are oriented in an oral direction, touching the setae of the Mx1-coxopodite. These setae belong to the posterior part of the ventral screen. The coxal endite also bears aborally curving serrulated setae (Fig. 4F). The denticles on these setae are about 6 μm long, becoming shorter towards the setal tip, giving it a cone-like appearance.

The medial rim of the endopodite consists of 800 μm long serrulated setae, 7 μm thick (Fig. 4A,B). There are plumose “leaf setae” with the overlapping flat setules on the anterior rim of the scaphognatite (Fig. 4G).

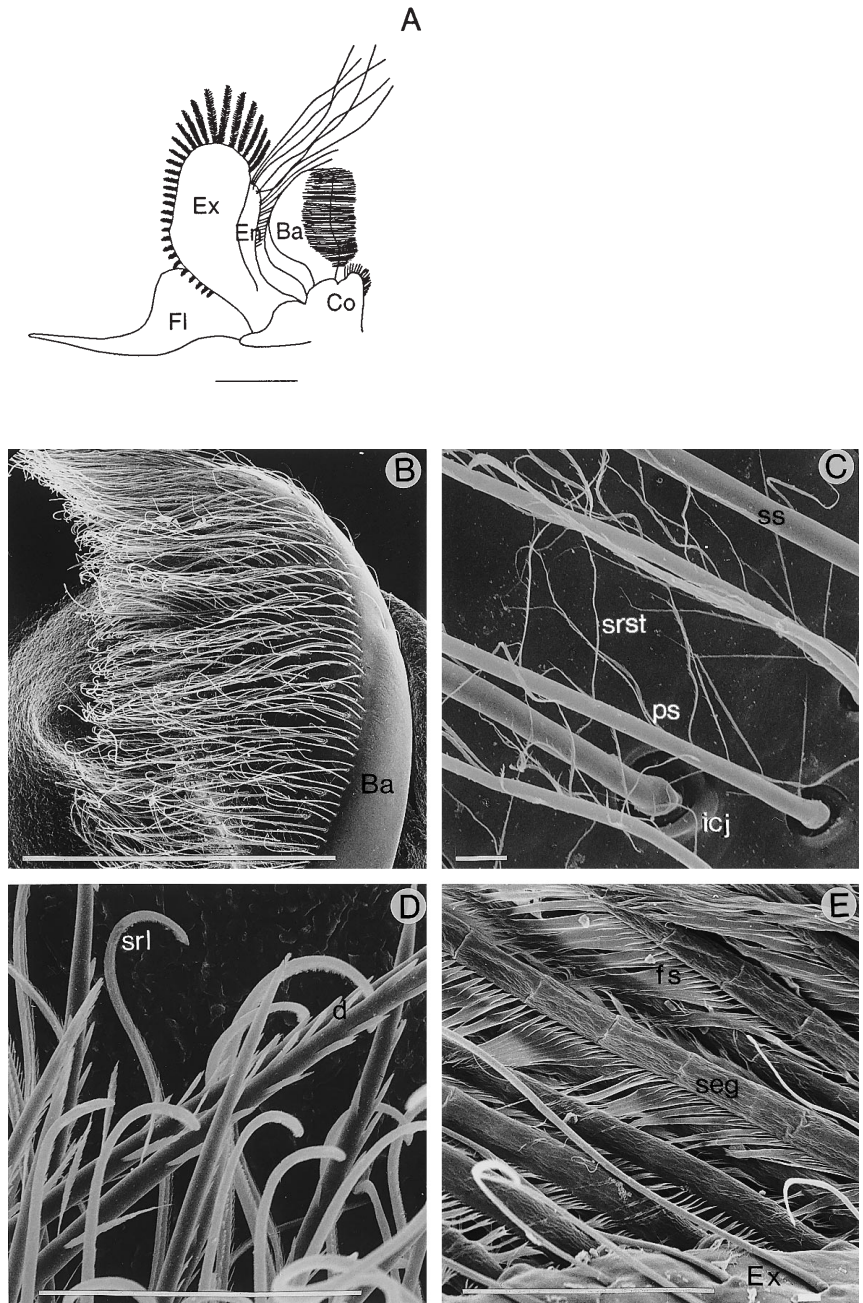
First maxilliped (MPI) (Fig. 5)

The first maxilliped is composed of a very small coxopodite, a voluminous curved basipodite, a flat endopodite, a leaf-shaped exopodite and a membranous flabellum (Fig. 5A). The setae on the medio-aboral side of basipodite are part of the ventral screen.

The basipodite’s aboral side is convex, the median half being densely packed with medially oriented setae (Fig. 5B) extending up to 400 μm over the medial rim. Two types of setae are present, both with infra-cuticular joints. Smooth simple setae, 500 μm long and 8 μm thick, are found mixed with thin pappose setae, 500 μm long and 2.5 μm thick. The pappose setae are sparsely

Fig. 5 *Callianassa subterranea*.

Morphology of the first maxilliped. **A** Line drawing of an aboral view. **B** SEM picture of the setose convex aboral side of basipodite (curling of setae is a preparation artefact). **C** Detail of proximal parts of basipodital setae. **D** Detail of the distal parts of the basipodital setae. **E** “Leaf-setae” fringing the exopodite. *Scale bars* = 1 mm (A, B); 100 μm (D); 10 μm (C, E) (*Co* coxopodite; *Ba* basipodite; *En* endopodite; *Ex* exopodite; *Fl* flabellum; *icj* infra-cuticular joints; *ps* thin pappose setae; *ss* thick simple setae; *srst* serrulated setules; *srl* rounded serrulate tips; *d* denticles; *seg* segmentation; *fs* flat overlapping setules)



covered with very fine, 30 μm long serrulated setules (Fig. 5C). The distal parts of the pappose setae are slightly serrulated with a rounded tip, the simple setae have denticles near the tip only (Fig. 5D). The setae and the setules compose a network with a mesh size of 20 to 30 μm .

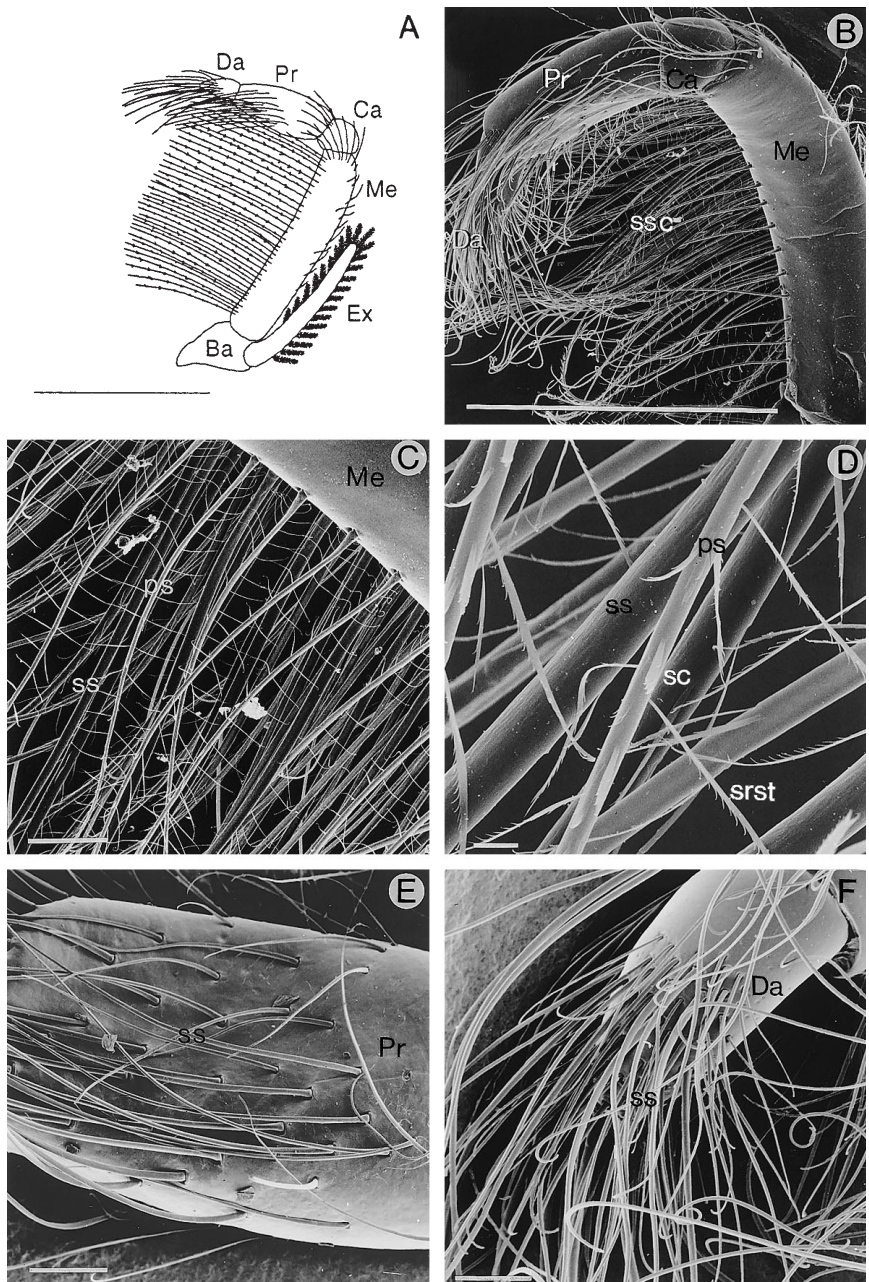
The flat endopodite has one row of 10 μm thick smooth setae with lengths between 500 and 1500 μm on the medial rim. Distally, a group of closely packed, very long (2000 to 2500 μm), 15 μm thick setae is found (Fig. 5A), sparsely covered with cylindrical setules.

The flat exopodite is fringed with a row of plumose "leaf setae" with lengths up to 800 μm , having flattened overlapping setules (Fig. 5E). The segmented, 15 μm thick setal shafts are implanted 30 to 70 μm apart.

Second maxilliped (MP2) (Fig. 6)

The second maxilliped consists of a base with a segmented pediform endopodite and a flat, slender, unsegmented exopodite (Fig. 6A). The endopodite is composed of a 1200 μm long meropodite with medially oriented long setae, a small carpopodite (about 250 μm long) with virtually no setae, a 650 μm long propodite with long setae, and a small, 250 μm long, dactylopodite with bundles of long setae (Fig. 6B). In a state of rest, the meropodite is positioned at an angle of about 30° to the lateral side relative to the body axis, the more distal segments are curved in a medial direction. The ventral setal screen is mainly composed of the setae on the meropodite. The exopodite is fringed by a rim of "leaf

Fig. 6 *Callianassa subterranea*. Morphology of the second maxilliped. **A** Line drawing of a view from the oral side. **B** SEM overview picture from the oral side. **C** Detail of the meropodital setal screen. **D** Fine detail of meropodital setae. **E, F** Details of the propodite and the dactylopodite. Scale bars = 1 mm (A, B); 100 μm (C, E, F); 10 μm (D) (*Ba* basis; *Ex* exopodite; *Me* meropodite; *Ca* carpopodite; *Pr* propodite; *Da* dactylopodite; *ssc* setal screen; *ss* simple setae; *ps* plumose setae; *sc* scales; *srst* serrated setules)



setae" (Fig. 6A). The medial rim of the meropodite has three to five rows of long setae, of the same two types as the MP1 basipodite: one or two rows of thin 800 μm long plumose setae (5 μm diameter) on the oral side, and two or three rows of equally long, 13 μm thick simple setae on the aboral side (Fig. 6C). Both setae types have infra-cuticular joints. The setae within one row are situated 70 μm apart, the setae of adjacent rows are implanted alternately. The plumose setae have 50 μm long serrulated setules on their lateral sides (Fig. 6D), which are attached almost perpendicular to the setal axis, about 35 μm apart (Fig. 6C,D). The setae on the meropodite's medial rim resemble a multi-layer net structure with an average mesh size of about 30 μm .

The propodite bears, mainly on the medio-oral side, 500 to 1000 μm long simple setae pointing in a distal direction (Fig. 6E). The oral side of the distal half of the dactylopodite is covered with a group of simple setae, 450 μm long and 8 μm thick, mixed with equally long, 15 μm thick rigid setae with finely serrated tips (Fig. 6F).

Third maxilliped (MP3) (Fig. 7)

The third maxilliped of *Callianassa subterranea* is by far its largest mouthpart, with a total length of up to 10 mm. It consists solely of a pediform segmented endopodite, an exopodite is lacking. At rest, the first two segments, the ischiopodite and the meropodite, are held at a small angle to the medial axis. The more distal segments, carpopodite, propodite and dactylopodite, point in a medio-ventral direction (Fig. 7A). The medio-oral side of the ischiopodite has a row of 11 to 13 large cuticular teeth, the "crista dentata", pointing in medial direction. The teeth are 200 to 300 μm high with tip-to-tip distances between 250 and 400 μm . All segments of the MP3 are richly supplied with setae, mainly on their medial and medio-ventral sides. The lateral sides of all segments are only sparsely covered with setae (Fig. 7B,C). The ischiopodite and the meropodite both have two types of setae on the medio-ventral rims. The aboral rows of setae are rigid and spine-shaped with a sharp tip, 900 μm long with a base diameter of 15 μm . The oral one or two rows of setae consist of very long, thin and flexible simple setae (1500 μm long, 10 μm thick), situated about 50 μm apart at right angles with the cuticula (Fig. 7B). (The curled appearance of these setae on the photographs is a preparation artefact. Untreated specimens studied with light microscopy showed that these setae are almost straight.) The oral sides of carpo-, pro- and dactylopodite are sparsely covered with identical long thin simple setae. The medio-ventral rim of the propodite also bears spine-shaped setae of about the same size as those on the meropodite, pointing in posterior direction when MP3 is at rest (Fig. 7B).

The dactylopodite is covered with loose rows of thin and long simple setae (800 μm long, 8 μm thick) and shorter thick simple setae (500 μm long, 20 μm thick),

the same two types as found on MP2's dactylopodite (Fig. 7D). In both types the distal part has lateral rows of scale-shaped denticles.

On the oral side of the propodite an oval group of densely packed serrated setae is situated (Fig. 7D), pointing distally. These setae have lengths between 50 and 200 μm and are strongly serrated over almost their entire length (Fig. 7E,F). Denticles of various shapes are found: straight, curved, sharp-pointed and blunt, which all point distally. The groove between the two rows of denticles was often found to contain small particles (Fig. 7G). The sides of the shafts opposite to the serration are covered with two rows of scales pointing in the same direction as the denticles. The distal rim of the carpopodite bears a few parallel rows of distally oriented setae of the same type as the propodites oval group.

Motion patterns during feeding

Both *mandibles* perform simultaneous repetitive medio-lateral movements at frequencies of 3 to 4 cycles s^{-1} (3 to 4 Hz). At the most medial position the toothed rims of the incisor processes touch. In the most lateral position the mouth opening is left free for food ingestion.

The *first maxillae* were often partly masked by more aborally situated mouthparts, but did not seem to move whenever they were visible.

The motion of the *second maxillae* could not be recorded on video, due to masking of the more aborally situated mouthparts. Binocular observations of one animal, however, showed that the basal endites make medio-lateral movements in phase with the mandibles.

The basipodites of both *first maxillipeds* also make simultaneous medio-lateral movements. The stroke in lateral direction is performed a little faster than the stroke in medial direction (Fig. 8A,B). At the lateralmost position, the basipodites rotate over a small angle along their longitudinal axes, moving the setal screens towards aboral. During the stroke to medial, the motion towards aboral is continued (Fig. 8B). At the medialmost position, the setal screens are lifted up, probably by rotating the basipodites back towards oral. Finally, the first maxillipeds move quickly back to lateral. The whole motion pattern is performed at the same frequency but in counter-phase with the mandibles and the second maxillae.

The *second maxillipeds* repetitively move simultaneously in medio-lateral direction (Fig. 9A,B), at the same frequency and in phase with the mandibles. During the lateral stroke the second maxillipeds are straightened, during the medial stroke, they are flexed (Fig. 9A). The second maxillipeds are rotating over small angles around the meropodites longitudinal axis during the stroke cycle. Due to these rotations, the setal screens of the meropodites become positioned at an angle with the plane of motion during the stroke towards medial. In the lateralmost position the setal screen is turned towards aboral. During the medial stroke the setae move through

Fig. 7 *Callianassa subterranea*. Morphology of the third maxilliped. **A** Line drawing of the oral side. **B** SEM picture of the oral side. **C** SEM picture of view from dorsal. **D** Detail of the oral sides of the propodite and dactylopodite. **E, F, G** Details of the propodites oval group of the serrated setae: setal bases (E) and scaled side setal tips (F); setal shafts, lateral denticles and scales (G). *Scale bars* = 1 mm (A, B, C, D); 10 μ m (E, F, G) (*Isch* ischiopodite; *Me* meropodite; *Ca* carpopodite; *Pr* propodite; *Da* dactylopodite; *cd* "crista dentata"; *og* oval group of serrated setae; *sps* spiny straight setae; *fss* flexible simple setae; *ssc* setal screen; *ss* simple setae; *ser* serration; *an* annulus; *sc* scales; *dt* denticles; *p* small particles)

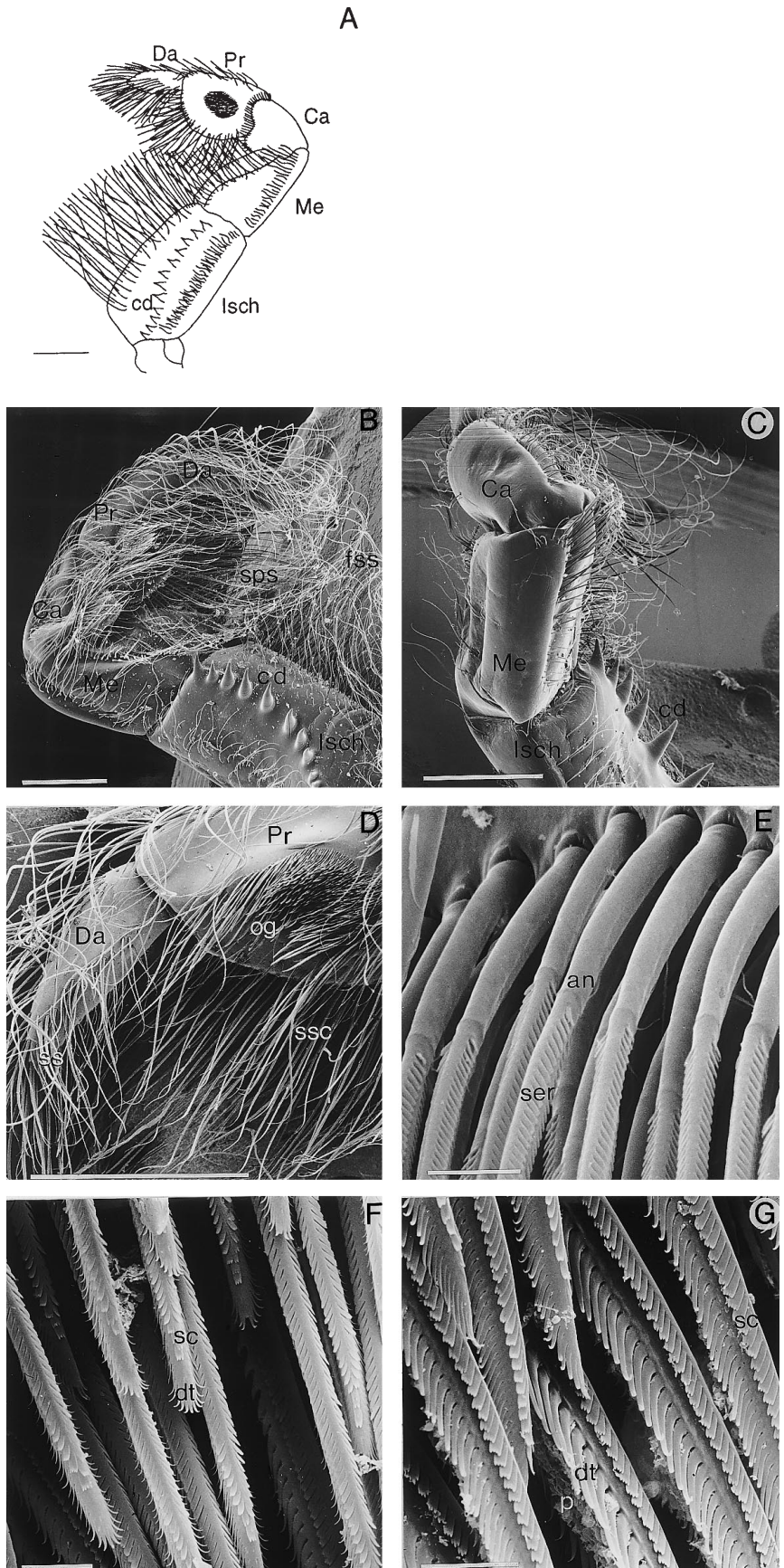
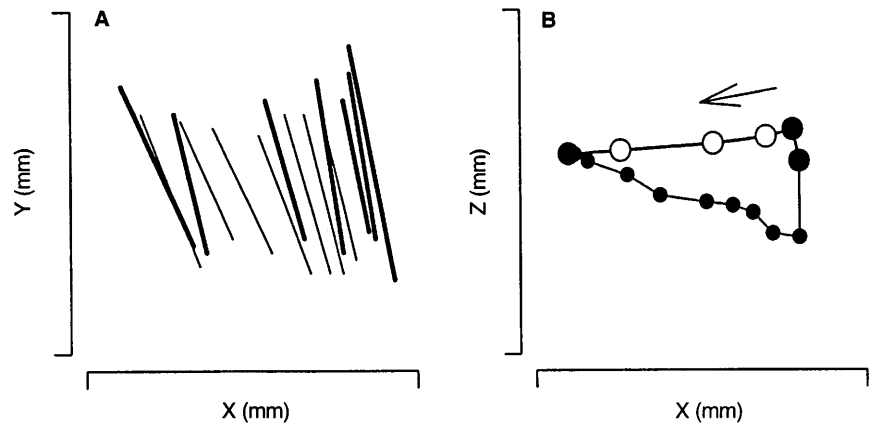


Fig. 8 *Callianassa subterranea*. Motion pattern of the right first maxilliped. *Thick lines* and *large dots* represent the lateral stroke; *thin lines* and *small dots* represent the medial stroke; *arrow* indicates direction of motion. **A** Wire frame diagram of subsequent positions of the basipodites medial rim, viewed from ventral, at 0.02-s intervals. **B** Motion cycle of the basipodites medial rim in the *XZ*-plane, viewed from rostral (top position is oralmost position); *open dots* are based on interpolated *Z*-positions



the fluid in front of the mouth and return to the plane of motion during the first part of the lateral stroke (Fig. 9C).

The movements of the left and right *third maxillipeds* alternate. These extremities flex during the medial and extend during the lateral stroke (Fig. 10A). The average frequency of the motion is about 1 Hz. The proximal segments (ischiopodite and meropodite) move only over small angles in the medio-lateral plane, whereas the more distal segments make larger excursions. In the lateralmost position, all segments line up and the third maxilliped is stretched to almost straight. During the medial stroke, the distal segments including the carpopodite swing in postero-medial direction. Flexing of all joints is performed almost simultaneously during this stroke. During the return stroke, the proximal segments of the third maxillipeds move in lateral direction first, followed by straightening of the more distal parts (Fig. 10A). The medial stroke is therefore not the inverse of

the lateral stroke (Fig. 10B). The third maxilliped moves in aboral direction at the start of the medial stroke, and is lifted up again during the last stage of the medial stroke (Fig. 10C), meanwhile interacting with the substrate. Because of the asymmetry of the motion cycle, sediment is accumulated and suspended directly in front of the other mouthparts and the mouth.

Phase relations between the movements of the mouthparts during feeding

The frequencies and phases of the moving mouthparts show a distinct pattern. The third maxillipeds make large excursions, and move alternately with a frequency of about 1 Hz. The second maxillipeds move simultaneously at 3 to 4 Hz, without an obvious phase-link with the third maxillipeds. The first maxillipeds move at a smaller amplitude than the second maxillipeds and

Fig. 9 *Callianassa subterranea*. Motion pattern of the endopodite of the right second maxilliped, view from aboral. *Thick lines* and *large dots* represent the lateral stroke; *thin lines* and *small dots* represent the medial stroke; *arrows* indicate the direction of motion. **A** Wire frame diagram of subsequent positions of the joints in the *XY*-plane, viewed from ventral, at 0.02-s intervals. Some points could not be registered during a part of the cycle, due to masking of other mouthparts. **B** Motion cycle of the tip in the *XY*-plane, viewed from ventral. **C** Motion cycle of the tip in the *XZ*-plane, viewed from rostral; the top of the figure is the oral side

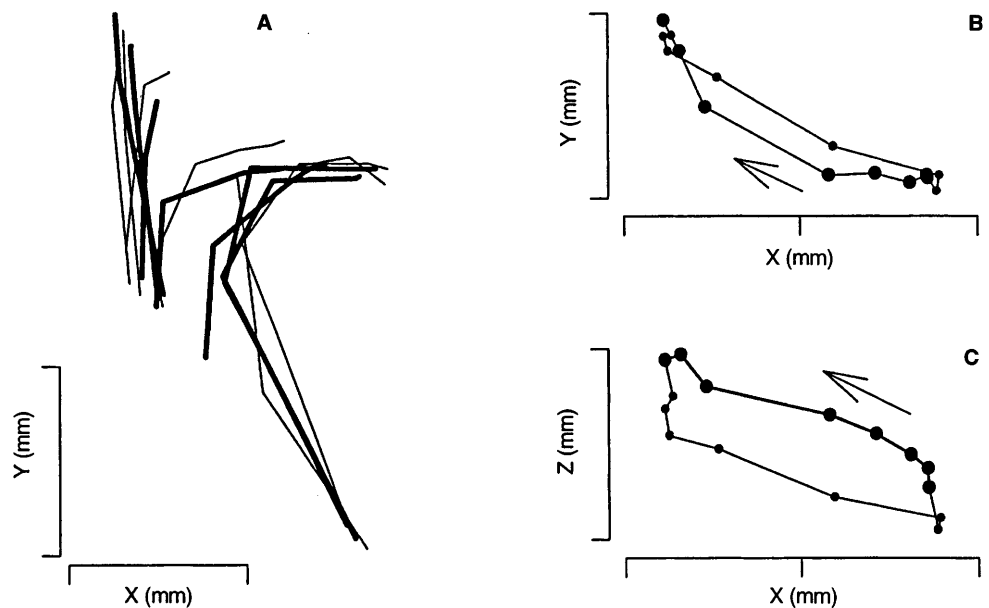
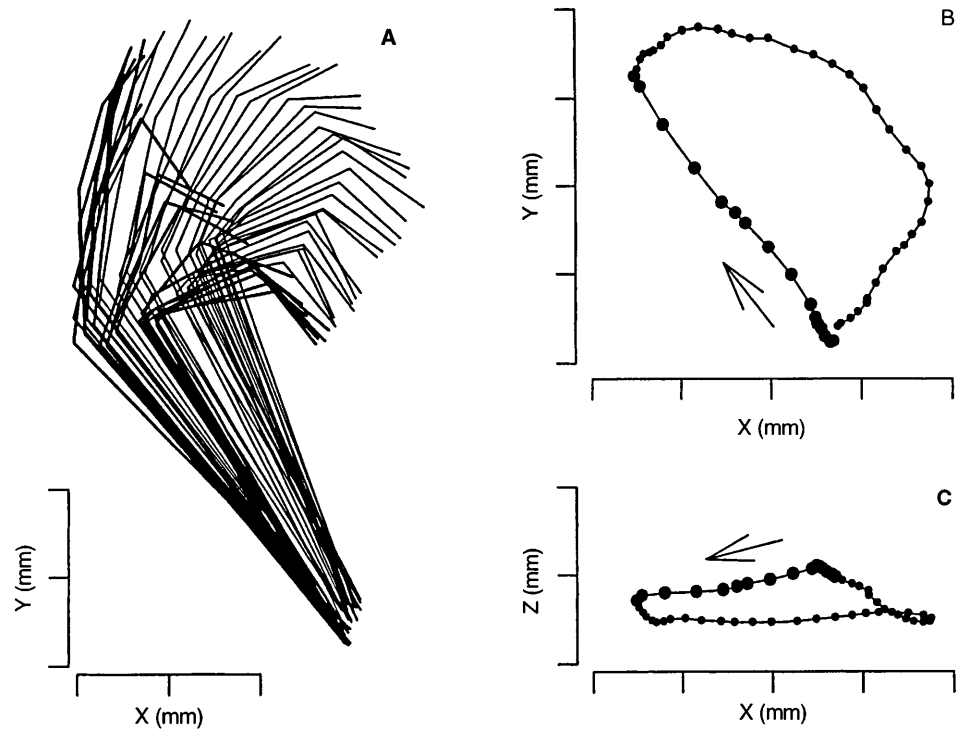


Fig. 10 *Callianassa subterranea*. Motion pattern of the right third maxilliped, view from aboral. *Thick lines and large dots* represent the lateral stroke; *thin lines and small dots* represent the medial stroke; *arrows* indicate the direction of motion. **A** Wire frame diagram of subsequent positions of the joints in the *XY*-plane, viewed from ventral, at 0.02-s intervals. **B** Motion cycle of the tip in the *XY*-plane, viewed from ventral. **C** Motion cycle of the tip in the *XZ*-plane, viewed from rostral; the top of the figure is the oral side



exactly in counter-phase. The second maxillae were observed to move at the same frequency and in phase with the second maxillipeds but in counter-phase with the first maxillipeds. The mandibles moved at the same frequency and in phase with the first maxillipeds but in counter-phase with the second maxillae. No motion of the first maxillae was recorded. Figure 11 shows an example of the lateral positions (*X*-direction) of the third, second and first left maxillipeds and the left mandible in time, to illustrate the described pattern.

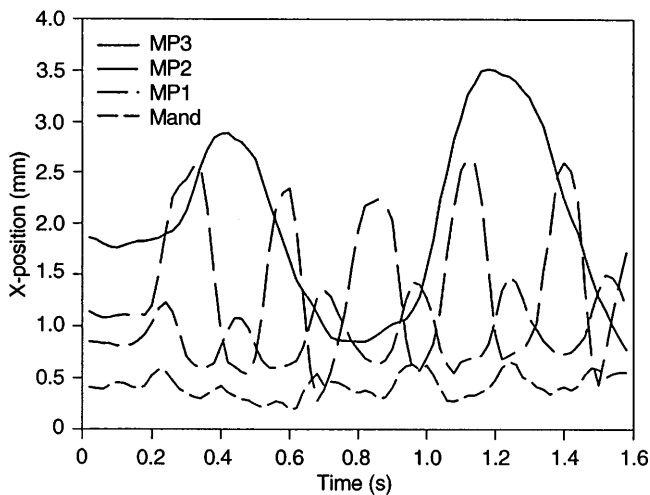


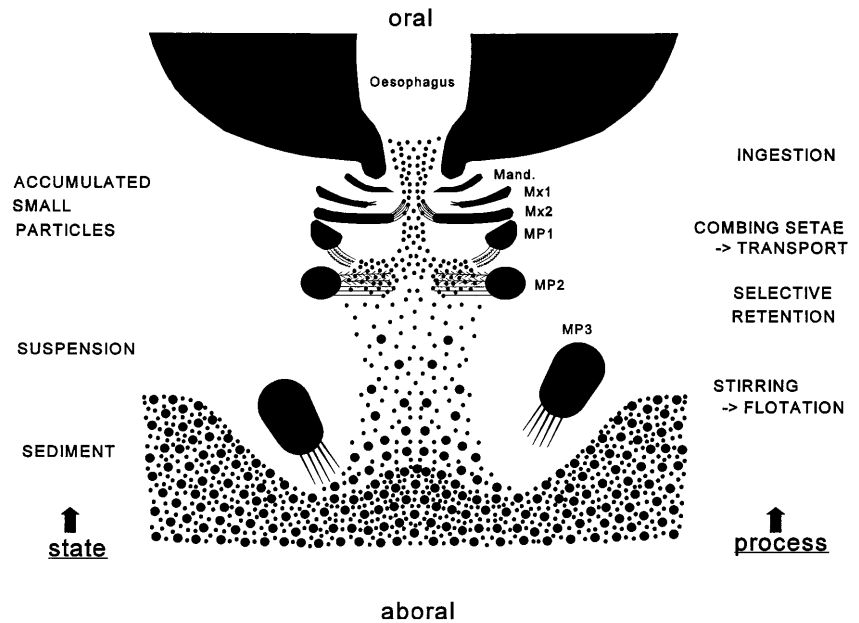
Fig. 11 *Callianassa subterranea*. *X*-positions versus time of the tips of the third and second maxillipeds, and of the medial rims of the first maxilliped and the mandible, showing their phase relations

The maxillipeds and the second maxillae also move in the oral–aboral direction (*Z*-direction in Figs. 8, 9, 10). The setal screens of the second as well as the first maxillipeds were recorded to move away from the mouth at the start of or during the medial stroke, and mouthwards at the start of or during the lateral stroke. Since all mouthparts except the third maxilliped’s lie closely packed in front of the mouth opening, the setal screens of the mouthparts interact. The first maxilliped’s basipodital setae were observed to comb through the second maxilliped’s meropodital setae when the first maxillipeds moved in the medial direction. The basipodital setae of the first maxillipeds moved in oral direction during the lateral stroke, moving in the opposite direction along the setal screens of the second maxillae. Combing of second maxillae setae through the first maxillipeds setae was not observed.

Callianassa subterranea’s feeding mechanism

The function of the mouthparts during feeding and the process of substrate selection are depicted in Fig. 12. During feeding, *C. subterranea* rejects coarse particles and ingests the fine fraction. The third maxillipeds accumulate sediment in front of the second maxillipeds by sweeping alternately through the top layer of the substrate. Sediment particles are suspended during the last phase of the medial stroke, when the third maxillipeds quickly turn in oral direction, producing a silty cloud in front of the other mouthparts. The second maxillipeds move through the upper layer of the suspension, trap-

Fig. 12 *Callianassa subterranea*. Schematic depiction of the feeding mechanism in a transversal cross section through the cephalo-thorax at the position of the oesophagus, showing the mouthparts, the processes and their compartments, and the state of the substrate, during feeding



ping the fine-grain fraction between the meropodital setae. The cloudiness disappears within seconds, and coarse particles are left behind. The fraction trapped by the second maxillipeds is combed out by the basipodital setae of the first maxillipeds. These particles accumulate on the oral side of the first maxillipeds' setal screen, and are taken over by the serrated setae of the second maxillae. During the last part of the medial stroke, the second maxillae probably push the accumulated particles into the mouth opening, when the mandibles are in their lateralmost position, leaving the mouth free for food ingestion. The sediment accumulated and suspended by the third maxillipeds is sorted during the process of feeding, and only the smaller, organically richer grain size fraction is ingested (Stamhuis et al. 1998). This selection process is performed in three steps: (1) size-dependent differences in flotation of the particles in the suspension result in the first sorting. A vertical particle-size gradient evolves in the suspension, because larger particles tend to sink faster than smaller particles. The second maxillipeds interact only with the upper layer of the suspension, containing mainly small particles. (2) The plumose setae on the medial rims of the second maxillipeds trap small particles from the suspension only. The second maxillipeds will selectively retain the particle size fraction of 30 μm and smaller, because the mesh-size of the meropodites' setal network is about 30 μm . (3) Finally, the particles retained by the second maxillipeds are transported to the mouth by the setal cascade of the other mouthparts. The distances among the setae involved in transporting the particles to the mouth are about 30 μm or less, and the setules or serrations enable handling of even smaller particles as well. There seems to be a constant negative selection on particles larger than about 30 μm during the whole feeding process, resulting in ingestion of the small particle fraction only.

Discussion

Callianassa subterranea is a selective deposit feeder. The structures on the mouthparts involved in food processing perform the selection of a particular particle fraction. However, the mouthparts of *C. subterranea* also show morphological structures not involved in deposit feeding, or of unclear function. The rim of large teeth on the medial sides of the third maxillipeds' meropodites (the "crista dentata"), the first maxillar basipodites with their teeth-like cuspidate setae, as well as the toothed medial ridges of the mandibles were not found to function in the selective deposit-feeding process. Since *C. subterranea*'s setal diversity is high, variations on the observed mechanism of feeding seem very well possible. The teeth-like structures enable clasping as well as shredding of larger food lumps (Thomas 1970; Caine 1974, 1975; Barker and Gibson 1977; Kunze and Anderson 1979). The other mouthparts might then be held in their lateralmost position, but they might also be involved in positioning of the food lump. The serrate setae of the second maxillae may be used to scrub or scratch organic matter from large lumps of material, e.g. gravel or remains of organisms. Nickell and Atkinson (1995) found *C. subterranea* to occasionally apply the third maxillipeds' crista dentata in cutting down lumps of silty sediment.

The smooth setae with the serrated tips on the second maxillae and the cuspidate setae of the first maxillae have a terminal pore, indicating that they might also function as chemoreceptors, providing additional food selection criteria (Shelton and Laverack 1970; Wiese 1976; Pohle and Telford 1981; Bush and Laverack 1982; Derby 1982; Gleeson 1982; Jacques 1989).

The scaphognatites of the second maxillae and the exopodites of the first and second maxillipeds bear a

special type of setae, also not directly involved in food processing. These plumose “leaf setae”, with closely packed flat setules in a fern-like arrangement, are assumed to generate and regulate water currents (Jacques 1989), e.g. for respiratory purposes (Farmer 1974; Pohle and Telford 1981; Schembri 1982a) or to rinse the mouthparts (Thomas 1970; Greenwood 1972; Farmer 1974; Kunze and Anderson 1979; Khan and Natarajan 1981; Felgenhauer and Abele 1983).

In general, a strong correlation exists between the functions of the mouthparts and the morphology of their setal structures (Wagner and Blinn 1987; Jacques 1989; Watling 1989). In *Callianassa subterranea*, the third maxillipeds stir up the sediment with brushes of firm simple setae. These setae do not clog due to their smoothness. The second maxillipeds selectively trap particles from the sediment suspension with plumose setae. This type of seta is found in many other filter- or suspension-feeding decapods, with similar function (Boltt 1961; Thomas 1970; Pohle and Telford 1981; Felgenhauer and Abele 1983; Wagner and Blinn 1987; Jacques 1989; Maitland 1990; Manjulatha and Babu 1991). The serrulations on the setules of the plumose setae increase adhesiveness, allowing the animal to effectively catch particles smaller than the setal mesh width (Wagner and Blinn 1987). The fragile plumose setae are lined by thick simple setae, probably to support them (Thomas 1970). The first maxillipeds take over the selected sediment fraction by combing through the plumose setae with pappose and simple setae. The pappose setae have serrulated setules to increase their adhesiveness (Wagner and Blinn 1987). The simple setae probably support the pappose setae (Thomas 1970). The second maxillae are assumed to transfer the fine particles from the first maxillipeds to the mouth opening, using scaled ear-like serrated setae. Serrated setae are, in general, used for scraping substrate, transferring material, holding objects and/or grooming (Pohle and Telford 1981), and scales on the shafts may be functional in improving grip on particulate matter. The scaled serrated setae on *C. subterranea*'s second maxillae as well as on the mandibular palps probably manipulate the selected fine-grained sediment fraction during the process of ingestion.

In *Callianassa subterranea*, a trend of decreasing passive motility of the setae on the mouthparts exists from aboral to oral, reflected by the type of joint (Jacques 1989). The setae on the aborally situated third and second maxillipeds, interacting with solid and suspended substrate, are long and flexible and have infra-cuticular joints. The more orally situated second maxillae, used for sediment manipulation, have stiff setae with supra-cuticular joints. This trend seems functional during feeding and food processing. Flexibility of the aboral setae prevents damage, and stiffness of the more oral setae probably increases their precision, preventing loss of food particles during the process of sorting and transporting sediment. The trend of a decreasing amplitude of motion of the mouthparts from aboral to oral

(Fig. 11) may be consistent with this, probably also indicating an increase in precision of particle handling towards oral. Similar sediment-processing mechanisms as determined for *C. subterranea* have been found in other decapods as well. Transporting particulate food to the mouth with alternately brushing mouthparts is found, e.g. in leucosid crabs (Schembri 1982a), hermit crabs (Khan and Natarajan 1981; Schembri 1982b) and galatheid prawns (Nicol 1932), but also within other crustacean orders (Manton 1977). In the amphibious semaphore crabs (*Uca* sp., *Heloeceus* sp.), the principle of flotation is also important in selection of particles with a high organic load, obtained from surface sediments (Miller 1961; Altevogt 1976; Maitland 1990). These crabs collect sediment with their chelipedes, and transport it to the mouthparts. The pre-oral cavity is then closed off with operculate third maxillipeds, after which the sediment is suspended with branchial water. As in *C. subterranea*, particles are captured from the suspension by the second and the first maxillipeds. These maxillipeds have “wooly hair”-like plumose setae as well as spoon-tipped setae for particle selection. The process of food acquisition is somewhat different from that of *C. subterranea*, due to the coarser substrate the crabs feed on. In the crabs, the plumose setae are used to trap small particles from the suspension. Additionally, the spoon-tipped setae are assumed to be able to scrape organic material from the coarse sediment particles originating from the beaches the crabs forage on at low tide (Altevogt 1957, 1976; Maitland 1990). Species foraging on coarser sediments appear to have more spoon-tipped setae and less plumose setae than species feeding on finer substrates (Miller 1961). *C. subterranea* lives in relatively silty sediments with about 12% (dry weight) of the substrate having a particle size of 30 µm or less (Stamhuis et al. 1998). Spoon-tipped setae for selection or scraping of larger grains are lacking on its maxillipedes, and selection is mainly accomplished by the plumose setae.

The morphology and motion patterns of *Callianassa subterranea*'s mouthparts and their functions during selective deposit feeding are consistent with other studies on its auto-ecology. The behaviour of this species is almost completely focussed on burrowing and sediment processing (Stamhuis et al. 1996), the morphology of its burrow has been related to a deposit-foraging life style (Griffis and Suchanek 1991; Nickell and Atkinson 1995; Rowden and Jones 1998; Stamhuis et al. 1997) and analysis of its stomach and gut contents showed fine-grained sediment with an increased organic content compared to unprocessed sediment (Stamhuis et al. 1998).

Acknowledgements We would like to thank E. Bosma for initially exploring the macro-morphology of the feeding appendages. We are grateful to M. Langevoord, P. van Nugteren and J. Smit for assisting in filming and analyzing the motions of the mouthparts. J. Zagers of the Laboratory of Electron Microscopy of the Dept. of Biology (University of Groningen) is acknowledged for introducing B.D. to SEM photography and preparing the final SEM-plates. We thank J. de Wiljes for maintaining the seawater systems.

References

- Alexander CG, Hindley JPR (1985) The mechanism of food ingestion by the banana prawn *Penaeus merguensis*. *Mar Behav Physiol* 12: 33–46
- Altevogt R (1957) Untersuchungen zur Biologie, Ökologie und Physiologie indischer Winkerkrabben. *Z Morph ökol Tiere* 46: 1–110
- Altevogt R (1976) Feeding apparatus and feeding process in Indian fiddler crabs: a SEM study. In: German scholars on Indian fiddler crabs. Nachiketa Publikations Ltd., Bombay, India, pp 1–13
- Barker PL, Gibson R (1977) Observations on the feeding mechanism, structure of the gut, and digestive physiology of the European lobster *Homarus gammarus* (L.) (Decapoda: Nephropidae). *J exp mar Biol Ecol* 26: 297–324
- Boltt RE (1961) Antennary feeding of the hermit crab *Diogenes brevisstris* (Stimpson). *Nature* 192: 1099–1100
- Bush BMH, Laverack MS (1982) Mechanoreception. In: Vernberg FJ, Vernberg WB (eds) *The biology of Crustacea*. Academic Press, New York, pp 399–456
- Caine EA (1974) Feeding of *Ovalipes guadulpensis* (Saussure) (Decapoda: Brachyura: Portunidae), and morphological adaptations to a borrowing existence. *Biol Bull mar biol Lab, Woods Hole* 147: 550–559
- Caine EA (1975) Feeding and masticatory structures of six species of the crayfish genus *Procambarus* (Decapoda, Astacidae). *Forma Functio* 8: 49–66
- Dale NG (1974) Bacteria in intertidal sediments: factors related to their distribution. *Limnol Oceanogr* 19: 509–518
- de Wilde PAWJ, Berghuis EM, Kok A (1984) Structure and energy demand of the benthic community of the Oyster Ground, Central North Sea. *Neth J Sea Res* 18: 143–159
- Derby CD (1982) Structure and function of cuticular sensilla of the lobster *Homarus americanus*. *J Crustacean Biol* 2: 1–21
- Derby CD (1989) Physiology of sensory neurons in morphologically identified cuticular sensilla of crustaceans. In: Felgenhauer BE, Thistle AB, Watling L (eds) *The functional morphology of feeding and grooming in Crustacea*. Balkema, Rotterdam, pp 27–40
- Factor JR (1978) Morphology of the mouthparts of larval lobsters, *Homarus americanus* (Decapoda: Nephropidae), with special emphasis on their setae. *Biol Bull mar biol Lab, Woods Hole* 154: 383–408
- Farmer AS (1974) The functional morphology of the mouthparts and periopods of *Nephrops norvegicus* (L.) (Decapoda: Nephropidae). *J nat Hist* 8: 121–142
- Felgenhauer BE, Abele LG (1983) Ultrastructure and functional morphology of feeding and associated appendages in the tropical fresh-water shrimp *Atya innocous* (Herbst) with notes on its ecology. *J Crustacean Biol* 3: 336–363
- Fenchel T (1972) Aspects of decomposer food chains in marine benthos. *Verh dt zool Ges* 65 (Sdhft): 15–22
- Fielder DR, Jones MB (1978) Observations of feeding behaviour in two New Zealand mud crabs (*Helice crassa* and *Macrophthalmus hirtipes*). *Mauri Ora* 6: 41–46
- Gemmell P (1979) Functional morphology of the feeding appendages of *Paratya australiensis* (Kemp) (Crustacea, Decapoda). *Zool Anz* 203: 129–138
- Gleeson RA (1982) Morphological and behavioral identification of the sensory structures mediating pheromone reception in the blue crab, *Callinectes sapidus*. *Biol Bull mar biol Lab, Woods Hole* 163: 162–171
- Greenwood JG (1972) The mouthparts and feeding behaviour of two species of hermit crabs. *J nat Hist* 6: 325–337
- Griffis RB, Suchanek TH (1991) A model of burrow architecture and trophic modes in thalassinidean shrimps (Decapoda: Thalassinidea) *Mar Ecol Prog Ser* 79: 171–183
- Jacques F (1989) The setal system of crustaceans: types of setae, groupings and functional morphology. In: Felgenhauer BE, Thistle AB, Watling L (eds) *The functional morphology of feeding and grooming in Crustacea*. Balkema, Rotterdam, pp 1–13
- Khan SA, Natarajan R (1981) Functional morphology of the mouthparts and feeding behaviour of the estuarine hermit crab *Clibanarius longitarsus* (De Haan). *Indian J mar Sci* 10: 357–362
- Kunze J, Anderson DT (1979) Functional morphology of the mouthparts and gastric mill in the hermit crabs *Clibanarius virescens* (Krauss), *Paguristes squamosus* (McCulloch) and *Dardanus setifer* (Milne-Edwards) (Anomura: Paguridae). *Aust J mar Freshwat Res* 30: 683–722
- Lopez GR, Levington JS (1987) Ecology of deposit-feeding animals in marine sediments. *Q Rev Biol* 62(3): 235–260
- Maitland DP (1990) Feeding and mouthpart morphology in the semaphore crab *Heloecius cordiformis* (Decapoda: Brachyura: Ocypodidae). *Mar Biol* 105: 287–296
- Manjulatha C, Babu DE (1991) Functional organisation of mouthparts and filter feeding in *Clibanarius longitarsus* (Crustacea: Anomura). *Mar Biol* 109: 121–127
- Manton SM (1964) Mandibular mechanisms and the evolution of Arthropoda. *Phil Trans R Soc* 247: 1–183
- Manton SM (1977) *The Arthropoda: habits, functional morphology and evolution*. Clarendon Press, Oxford
- Miller DC (1961) The feeding mechanism of fiddler crabs, with ecological considerations of feeding adaptations. *Zoologica NY* 46: 89–100
- Nickell LA, Atkinson RJA (1995) Functional morphology of burrows and trophic modes of three thalassinidean shrimp species, and a new approach to classification of thalassinidean burrow morphology. *Mar Ecol Prog Ser* 128: 181–197
- Nicol EAT (1932) The feeding habits of the *Galatheaidea*. *J mar biol Ass UK* 18: 97–106
- Pohle G, Telford M (1981) Morphology and classification of decapod crustacean larval setae: a scanning electron microscopy study of *Dissodactylus crinitichelis*, Moreira, 1901 (Brachyura: Pinnotheridae). *Bull mar Sci* 31: 736–752
- Roberts MH (1968) Functional morphology of the mouthparts of the hermit crabs *Pagurus longicarpus* and *Pagurus pollicaris*. *Chesapeake Sci* 6: 9–20
- Robertson JR, Newell SY (1982a) A study of particle ingestion by three fiddler crab species foraging on sandy sediments. *J exp mar Biol Ecol* 65: 11–17
- Robertson JR, Newell SY (1982b) Experimental studies of particle ingestion by the sand fiddler crab *Uca pugilator* (Bosc). *J exp mar Biol Ecol* 59: 1–21
- Rowden AA, Jones MB (1998) Sediment turnover estimates for the mud shrimp *Callinassa subterranea* [Montagu] (Thalassinidea) and its influence upon resuspension in the North Sea. *Contin Shelf Res* (in press)
- Schembri PJ (1982a) The functional morphology of the feeding and grooming appendages of *Ebalia tuberosa* (Pennant) (Crustacea: Decapoda: Leucosiidae). *J nat Hist* 16: 467–480
- Schembri PJ (1982b) Functional morphology of the mouthparts and associated structures of *Pagurus rubricatus* (Crustacea: Decapoda: Anomura) with special reference to feeding and grooming. *Zoomorphology* 101: 17–38
- Shelton RG, Laverack MS (1970) Receptor hair structure and function in the lobster *Homarus gammarus* (L.). *J exp mar Biol Ecol* 4: 201–210
- Skilleter GA, Anderson DT (1986) Functional morphology of the chelipeds, mouthparts and gastric mill of *Ozius truncatus* (Milne-Edwards) (Xanthidae) and *Leptograpsus variegatus* (Fabricius) (Grapsidae) (Brachyura). *Aust J mar Freshwat Res* 37: 67–79
- Stamhuis EJ, Reede-Dekker T, van Etten Y, de Wiljes JJ, Videler JJ (1996) Behaviour and time allocation of the burrowing shrimp *Callinassa subterranea* (Decapoda, Thalassinidea). *J exp mar Biol Ecol* 204: 225–239
- Stamhuis EJ, Schreurs CE, Videler JJ (1997) Burrow architecture and turbative activity of the thalassinid shrimp *Callinassa subterranea* from the central North Sea. *Mar Ecol Prog Ser* 151: 155–163

- Stamhuis EJ, Videler JJ, de Wilde PAJW (1998) Optimal foraging in the thalassinid shrimp *Callinassa subterranea*: improving food quality by selection on grain size. *J exp mar Biol Ecol* (in press)
- Taghon GL (1982) Optimal foraging by deposit-feeding invertebrates: roles of particle size and organic coating. *Oecologia* 52: 295–304
- Taghon GL, Self RL, Jumars PA (1978) Predicting particle selection by deposit feeders: a model and its implications. *Limnol Oceanogr* 23: 752–759
- Thomas WJ (1970) The setae of *Austropotamobius pallipes* (Crustacea: Astacidae). *J Zool Lond* 160: 91–142
- Thomas WJ (1973) The hatchling setae of *Austropotamobius pallipes* (Lereboullet) (Decapoda: Astacidae). *Crustaceana* 24: 77–89
- Wagner VT, Blinn DW (1987) A comparative study of the maxillary setae for two coexisting species of *Hyalella* (Amphipoda), a filter feeder and a detritus feeder. *Arch Hydrobiol* 109: 409–419
- Watling L (1989) A classification system for crustacean setae based on the homology concept. In: Felgenhauer BE, Thistle AB, Watling L (eds) *The functional morphology of feeding and grooming in Crustacea*. Balkema, Rotterdam, pp 15–26
- Weise W, Rheinheimer G (1978) Scanning electron microscopy and epifluorescence investigation of bacterial colonization of marine sand sediments. *Microb Ecol* 4: 175–188
- Wiese K (1976) Mechanoreceptors for near-field water displacement in crayfish. *J Neurophysiol* 39: 816–833